Inorg. Chem. **1997,** *36,* 2944−2949

Synthesis and Coordination Chemistry of the Bis(imidazole) Ligand, Bis(1-methyl-4,5-diphenylimidaz-2-oyl)(benzyloxy)methane

Rajiv Bhalla, Madeleine Helliwell, and C. David Garner*

The Chemistry Department, University of Manchester, Oxford Road, Manchester, M13 9PL U.K.

Received October 2, 1996[⊗]

The synthesis and characterization of the new imidazole ligand bis(1-methyl-4,5-diphenylimidaz-2-oyl)(benzyloxy)methane (BimOBz) and its copper(II) complexes $[Cu(BimOBz)_2][BF_4]_2 \cdot 2H_2O$ ($\mathbf{1} \cdot 2H_2O$), $[Cu(BimOBz)(NO_3)_2] \cdot CH_2Cl_2$ ($\mathbf{2} \cdot CH_2Cl_2$) and $[Cu(BimOBz)Cl_2] \cdot 2EtOH$ ($\mathbf{3} \cdot 2EtOH$) are presented. The X-ray crystallographic parameters determined are as follows: $\mathbf{1} \cdot$solv (solv = petroleum ether) $C_{84}H_{66}N_8B_2CuF_8O_2$, 1456.65, monoclinic space group ($P2_1/a$), $a = 20.862(8)$ Å, $b = 19.110(5)$ Å, $c = 22.452(9)$ Å, $\beta = 110.09(3)°$, $Z = 4$, $R = 0.129$, and $R_w = 0.139$. $\mathbf{2} \cdot CH_2Cl_2$, $C_{41}H_{36}N_6Cl_2O_7$, 859.22, monoclinic space group ($P2_1/c$), $a = 9.748(1)$ Å, $b = 14.157(5)$ Å, $c = 17.209(2)$ Å, $\beta = 103.709(8)°$, $Z = 4$, $R = 0.066$, and $R_w = 0.087$. $\mathbf{3} \cdot 2EtOH$, $C_{44}H_{38}N_4Cl_2CuO_2$, 789.26, monoclinic space group ($P2_1/a$), $a = 17.171(5)$ Å, $b = 13.988(3)$ Å, $c = 17.897(5)$ Å, $\beta = 112.52(2)°$, $Z = 4$, $R = 0.084$, and $R_w = 0.092$. The geometry at these Cu^{II} centers is distorted tetrahedral in **1** and **3** and essentially square-planar in **2**, and this difference is reflected in their EPR spectra, especially the value of A_z; **1** (solid, $g_x = 2.06$, $g_y = 2.13$, $g_z = 2.30$, $A_z = 94 \times 10^{-4}$ cm^{-1}), **3** (CH_2Cl_2, 77 K, $g_x = g_y = 2.06$, $g_z = 2.37$, $A_z = 75 \times 10^{-4}$ cm^{-1}), **2** (solid, $g_x = g_y = 2.06$, $g_z = 2.28$, $A_z = 169 \times 10^{-4}$ cm^{-1}). **1** displays a reversible, one-electron Cu^{II}/Cu^{I} couple in CH_2Cl_2 and MeCN at potentials of +0.62 and +0.49 V vs SCE, respectively.

Introduction

The role of the metal center at the active sites of copper proteins has been the focus of much attention for both synthetic and biological chemists. The active site structures of these proteins usually involve copper coordinated to at least two histidine imidazole groups.[1−7] The oxidized form of Cu/Zn bovine superoxide dismutase possesses a copper center coordinated to three histidine imidazoles and one histidine imidazolate group; the imidazolate group bridges the copper to a zinc^{II} ion.[4] The geometry of the $Cu^{II}N_4$ unit is considerably removed from square-planar; X-ray crystallographic studies have shown that the geometry of the copper center is essentially retained upon reduction in the solid state,[8] but NMR[9] and EXAFS[10] studies indicate that the Cu^{I} center is three-coordinate in solution.

These naturally occurring copper centers have stimulated much research into the design and synthesis of chemical analogs. The ubiquity of the imidazole groups of the amino acid histidine in the coordination sphere of copper proteins[1−7] has necessitated that ligands should contain a donor group that mimics the histidine imidazole. While imidazole is the obvious choice, the difficulty of incorporating the imidazole group into a chelating ligand has often resulted in the use of other nitrogen donors, especially aromatic nitrogen donors (pyridine, pyrazole).[11−13] Although pyridine has electronic properties similar to imidazole, it is larger than imidazole. In contrast, the pyrazole group is of a similar size, but is considerably more basic ($pK_a = 14.2$ vs 7.2). The abiological nature of the pyrazole (and pyridine) group has prompted the synthesis of poly(imidazole) ligands.[14−18] As a contribution to this topic, we have synthesized[19−21] a series of bis- and tris(imidazole) ligands. Also, we have recently reported the synthesis of bis(1-methyl-4,5-diphenylimidaz-2-oyl)carbinol (BimOH) and the tetracopper complex $[Cu_4(BimOH)_2(BimO)_2][PF_6]_4$.[21b] For the work reported herein, the conversion of the alcohol functionality of BimOH to produce bis(1-methyl-4,5-diphenylimidaz-2-oyl)(benzyloxy)methane BimOBz (Scheme 1) was accomplished in order to remove the option of the deprotonation to give an alkoxide, which could be a strong competitor of the imidazole for coordination sites on a metal ion such as Cu^{II}.

[⊗] Abstract published in *Advance ACS Abstracts*, May 15, 1997.

(1) Guss, J. M.; Merritt, E. A.; Phizackerly, R. P.; Hedman, B.; Murata, M.; Hodgson, K. O.; Freeman, H. C. *Science* **1988**, 241, 806.

(2) Baker, E. N. *J. Mol. Biol.* **1983**, *203*, 1071.

(3) Magnus, K. A.; Ton-That, H.; Carpenter, J. E. *Chem. Rev.* **1994**, *94*, 727.

(4) Tainer, J. A.; Getzoff, E. D.; Beem, K. M; Richardson, J. S.; Richardson, D. C. *J. Mol. Biol.* **1982**, *160*, 181.

(5) Ito, N.; Philips, S. E. V.; Stevens, C.; Oqel, Z. P.; McPherson, M. J.; Keen, J. N.; Yadav, K. D. S.; Knowles, P. F. *Nature (London)* **1991**, *350*, 87.

(6) Godden, J. W.; Turley, S.; Teller, D. C.; Adman, E. T., Liu, M.-Y.; LeGall, J. *Science* **1991**, *253*, 438.

(7) Messerschmidt, A.; Rossi, A.; Ladenstein, R.; Huber, R.; Bolognesi, M.; Gatti, G.; Manchesini, A.; Petruzelli, R.; Finazzo-Agnó, A. *J. Mol. Biol.* **1989**, *206*, 513.

(8) Rypniewski, W. R.; Mangani, S.; Bruni, B.; Orioli, P. L.; Casati, M.; Wilson, K. S. *J. Mol. Biol.* **1995**, *251*, 282.

(9) Bertini, I.; Banci, L.; Luchinat., C; Piccioli, M. *Coord. Chem. Rev.* **1990**, *100*, 67.

(10) Blackburn, N. J.; Hasnain, S. S.; Binsted, N.; Diakun, G. P.; Garner, C. D.; Knowles, P. F. *Biochem. J.* **1984**, *219*, 985.

(11) Tyeklar, Z; Karlin, K. D. *Acc. Chem. Res.* **1989**, *22*, 241.

(12) Kitajima, N. *Adv. Inorg. Chem.* **1992**, *39*, 1.

(13) Kitajima, N.; Fujisawa, K.; Moro-oka, Y. *J. Am. Chem. Soc.* **1990**, *112*, 3210.

(14) Bouwmann, E.; Driessen, W. L.; Reedijk, J. *Coord. Chem. Rev.* **1990**, *104*, 143.

(15) Tran, K. C.; Battioni, J. P., Zimmermann, J. L.; Bois, J. Koolhaas, G. J. A. A.; Leduc, P.; Mulliez, E.; Boumchita, H.; Reedijk, J.; Chottard, J. C. *Inorg. Chem.* **1994**, *33*, 2808.

(16) Chen, S.; Richardson, J. F.; Buchanan, R. M. *Inorg. Chem.* **1994**, *33*, 2376.

(17) Sorrell, T. N.; Allen, W. E.; White, P. S. *Inorg. Chem.* **1995**, *34*, 952.

(18) Lynch, W. E.; Kurtz, D. M., Jr.; Wang. S; Scott, R. A. *J. Am. Chem. Soc.* **1994**, *116*, 11030.

(19) Higgs, T. C.; Helliwell, M.; Garner, C. D. *J. Chem. Soc., Dalton Trans.* **1996**, 2101.

(20) McMaster, J.; Beddoes, R. L.; Collison, D.; Eardley, D. R.; Helliwell, M.; Garner, C. D. *Chem. Eur. J.* **1996**, *2*, 685.

(21) (a) Bhalla, R.; Collison, D.; Helliwell, M.; Garner, C. D., submitted to *Inorg. Chim. Acta.* (b) Bhalla, R.; Helliwell, M.; Garner, C. D. *J. Chem. Soc., Chem. Commun.* **1996**, 921.

S0020-1669(96)01204-9 CCC: $14.00

Scheme 1. Synthesis of Bis(1-methyl-4,5-diphenylimidaz-2-oyl)(benzyloxy)methane

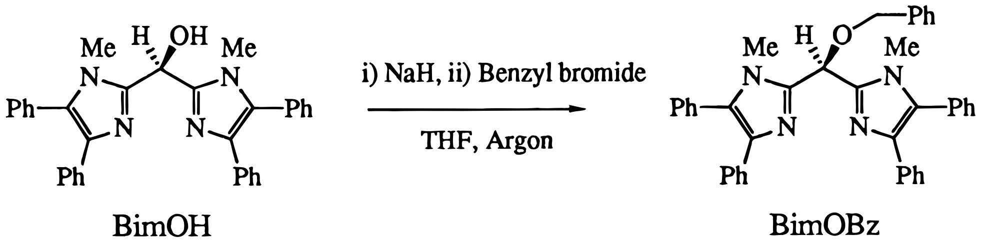

Experimental Section

Synthesis. Bis(1-methyl-4,5-diphenylimidaz-2-oyl)carbinol was prepared according to procedures described by Bhalla *et al.*[21a] All other reagents were obtained from Aldrich Chemical Co. and used without further purification. Tetrahydrofuran was distilled from sodium/benzophenone.

Bis(1-methyl-4,5-diphenylimidaz-2-oyl)(benzyloxy)methane (BimOBz). Bis(1-methyl-4,5-diphenylimidaz-2-oyl)carbinol (3.0 g, 6.0 mmol) was placed in a 3-necked 500 cm^3 round-bottomed flask. The flask was purged and filled with argon. Dry, degassed THF (80 cm^3) was then added via a syringe. Sodium hydride (80% dispersion in mineral oil, 0.36 g, 12.0 mmol) was added to the suspension, which was stirred at room temperature for 30 min, in order to effect complete deprotonation, during which time a pale yellow solution formed. Benzyl bromide (1.5 cm^3, 12.6 mmol) was then carefully added to the reaction via syringe. The reaction mixture was stirred at room temperature overnight, during which time a fine white precipitate formed. The excess NaH was destroyed by the careful addition of *i*-PrOH/EtOH (2:1 v/v) (20 cm^3). The pale yellow solution was transferred to a separating funnel and washed with distilled water (2 × 50 cm^3). The aqueous phase was then washed with CH_2Cl_2 (2 × 20 cm^3). The organic fractions were combined and the solvents removed under vacuum, yielding a pale yellow oil. This was dissolved in CH_2Cl_2 (100 cm^3) and dried over anhydrous $MgSO_4$, which was collected by filtration and washed with CH_2Cl_2 (2 × 20 cm^3). The filtrate and the washings were combined, and the volume was reduced by half under vacuum. The solution was placed in a crystallizing dish, together with absolute EtOH (20 cm^3). Colorless crystals formed which were collected by filtration, washed with absolute EtOH (20 cm^3), and dried under vacuum. Yield: 2.8 g (79%). Mp: 208−210 °C. ^{1}H NMR (300 MHz, $CDCl_3$): δ 3.5 (s, 6 H, NCH_3), 4.8 (s, 2 H, CH_2), 6.2 (s, 1 H, CHOBz), 7.1−7.65 (m, 25 H, ArH). Anal. Calcd for $C_{40}H_{34}N_4O$ (MW 586.73): C, 81.9; H, 5.8; N, 9.6. Found: C, 80.1; H, 6.4; N, 9.2. MS observed parent (EI/CI) 586 (M^+ 586).

$[Cu(BimOBz)_2][BF_4]_2\cdot 2H_2O$ ($1\cdot 2H_2O$). A solution of $Cu(BF_4)_2\cdot 4.5H_2O$ (0.055 g, 0.17 mmol) in absolute EtOH (10 cm^3) was added dropwise to a colorless solution of BimOBz (0.20 g, 0.34 mmol) in CH_2Cl_2 (20 cm^3). This resulted in the instantaneous formation of an intense green solution which was stirred at room temperature for 1 h, at the end of which time a blue/green solution was obtained. Blue crystals formed overnight which were collected by filtration, washed with absolute EtOH (20 cm^3), and dried under vacuum. Yield: 0.19 g (77%). Anal. Calcd for $C_{80}H_{72}N_8B_2CuF_8O_4$ (MW 1446.65): C, 66.4; H, 5.0; N, 7.7; B, 1.5; Cu, 4.4. Found: C, 64.2; H, 4.9; N, 7.4; B, 1.5; Cu, 3.9. MS (+FAB) $(BimOBz)^+$, 586; $[Cu(BimOBz)]^+$, 649; $[Cu(BimOBz)_2]^+$, 1237.

$[Cu(BimOBz)(NO_3)_2]$. CH_2Cl_2 ($2\cdot CH_2Cl_2$). A solution of $Cu(NO_3)_2\cdot 3H_2O$ (0.08 g, 0.33 mmol) in absolute EtOH (10 cm^3) was added dropwise to a colorless solution of BimOBz (0.20 g, 0.34 mmol) in CH_2Cl_2 (20 cm^3). Initially, this resulted in the formation of a pale blue solution which eventually changed to an intense green on stirring at room temperature for 1 h. Pale blue crystals formed which were collected by filtration, washed with absolute EtOH (20 cm^3), and dried under vacuum. Yield: 0.20 g (68%). Anal. Calcd for $C_{41}H_{36}N_6Cl_2CuO_7$ (MW 859.22): C, 57.3; H, 4.2; N, 9.8; Cu, 7.4. Found: C, 57.8; H, 4.3; N, 9.5; Cu, 7.1. MS (+FAB) $(BimOBz)^+$, 586; $[Cu(BimOBz)]^+$, 649; $[Cu(BimOBz)(NO_3)]^+$, 711.

$[Cu(BimOBz)Cl_2]$ (3). A solution of $CuCl_2\cdot 3H_2O$ (0.08 g, 0.33 mmol) in absolute EtOH (10 cm^3) was added dropwise to a colorless solution of BimOBz (0.20 g, 0.34 mmol) in CH_2Cl_2 (20 cm^3). This resulted in the formation of a red/brown solution initially which changed to green color on complete addition. The solution was allowed to stir at room temperature for 1 h. Orange crystals formed on standing at room temperature overnight which were collected by filtration, washed with absolute EtOH (20 cm^3), and dried under vacuum. Yield: 0.19 g (75%). Anal. Calcd for $C_{40}H_{34}N_4Cl_2CuO$ (MW 721.20): C, 66.6; H, 5.0; N, 7.8; Cl, 9.8; Cu, 8.8. Found: C, 65.3; H, 4.8; N, 7.6; Cl, 9.6; Cu, 7.9. MS (+FAB) $(BimOBz)^+$, 586; $[Cu(BimOBz)]^+$, 649; $[Cu(BimOBz)Cl]^+$, 684.

Table 1. Crystallographic Data for **1**·solv, **2**·CH_2Cl_2, and **3**·2EtOH

	$C_{84}H_{66}N_8B_2CuF_8O_2$		
a, Å	20.862(8)	space group	$P2_1/a$
b, Å	19.110(5)	T, K	296
c, Å	22.452(9)	Cu Kα (λ, Å)	1.541 78
β, deg	110.09(3)	D_{calcd}, g cm^{-1}	1.151
V, Å^3	8407(6)	μ, cm^{-1}	8.83
Z	4	R^a	0.129
MW	1456.65	$R_w{}^b$	0.139
	$C_{41}H_{36}N_6Cl_2CuO_7$		
a, Å	9.748(1)	space group	$P2_1/c$
b, Å	14.157(5)	T, K	296
c, Å	17.209(2)	Cu Kα (λ, Å)	1.541 78
β, deg	103.709(8)	D_{calcd}, g cm^{-1}	1.449
V, Å^3	3937(1)	μ, cm^{-1}	25.21
Z	4	R^a	0.066
MW	859.22	$R_w{}^b$	0.087
	$C_{44}H_{38}N_4Cl_2CuO_2$		
a, Å	17.171(5)	space group	$P2_1/a$
b, Å	13.988(3)	T, K	296
c, Å	17.897(5)	Cu Kα (λ, Å)	1.541 78
β, deg	112.52(2)	D_{calcd}, g cm^{-1}	1.320
V, Å^3	3971(2)	μ, cm^{-1}	23.44
Z	4	R^a	0.084
MW	789.26	$R_w{}^b$	0.092

[a] $R = \sum||F_o| - |F_c||/\sum|F_o|$. [b] $R_w = [(\sum w(|F_o| - |F_c|)^2/\sum wF_o^2)]^{1/2}$; $w = 4F_o^2/\sigma^2(F_o^2)$.

Crystallographic Data Collection and Refinement of the Structures. A summary of the crystallographic data is presented in Table 1. Data were collected on a Rigaku AFC5R diffractometer with graphite-monochromated Cu Kα radiation and a 12 kW rotating anode generator at room temperature using the $\omega/2\theta$ scanning technique. The structures were solved by Patterson methods using the SHELXS-86 program.[22] The data in each case were corrected for absorption, Lorentz and polarization effects using the DIFABS program.[23] The intensities of three representative reflections were measured after every 150 reflections, and a linear correction factor was included to account for any decay. In each case, the function minimized during full-matrix, least-squares refinement was $\sum w(|F_o| - |F_c|)^2$, using standard neutral-atom dispersion factors and anomalous dispersion corrections.[24] Hydrogen atoms were placed in idealized positions (C−H = 0.95 Å) and were assigned isotropic thermal parameters that were 20% greater than

---

(22) Sheldrick, G. M. *SHELXS-86 in Crystallographic Computing 3*; Sheldrick, G. M., Kreuger, C., Goddard, R., Eds.; Oxford University Press: New York, 1985; p 175.

(23) Walker, N.; Stuart, D. *Acta Crystallogr.* **1983**, *A39*, 158.

(24) (a) Cromer, D. T.; Waber, J. T. *International Tables for X-ray Crystallography*; The Kynoch Press: Birmingham, England, 1974; Vol. IV, Table 2.2A. (b) Cromer, D. T. *International Tables for X-ray Crystallography*; The Kynoch Press: Birmingham, England, 1974; Vol. IV, Table 2.3.1.

the equivalent *B* value of the atom to which they were bonded. Least-squares planes were calculated using the PLATON program.[25]

Crystals of **1**·solv were grown by solvent layering. The compound was dissolved in CH_2Cl_2 and transferred to a Pasteur pipet, flame sealed at one end. Five times the volume of 60−80 petroleum ether was then carefully layered onto the solution. The pipet was then completely sealed. After several days, blue blocklike crystals suitable for X-ray diffraction studies formed at the interface. A crystal was selected and mounted on a glass capillary and coated with an epoxy resin due to its solvent sensitivity. The structure was refined in the non-standard setting $P2_{1/a}$ of the space group $P2_{1/c}$. The asymmetric unit consists of the copper-containing cation and two $[BF_4]^-$ anions. Also present were a number of solvent fragments (probably disordered 60−80 petroleum ether) with an atom occupancy of a 0.5. The phenyl ring carbons and the non-hydrogen atoms of the solvent fragments were refined isotropically since there were insufficient data to refine all of the atoms anisotropically. Initially, the $[BF_4]^-$ anions were treated as rigid groups, but in the later stages of refinement, the fluorine atoms were refined anisotropically with the boron atoms fixed in their idealized positions and refined isotropically. The remaining non-hydrogen atoms were refined anisotropically. The final full-matrix least-squares refinement converged with $R = 0.129$ and $R_w = 0.139$. The high *R* value is a attributed primarily to the disordered $[BF_4]^-$ anions and the solvent fragments. The maximum and minimum peaks on the final difference Fourier map corresponded to 0.59 and −0.44 e $Å^{-3}$.

Green tabular crystals of **2**·CH_2Cl_2 suitable for crystallographic investigations were grown by evaporation from a CH_2Cl_2/EtOH solution. In addition to one molecule of $[Cu(BimOBz)(NO_3)_2]$, a CH_2Cl_2 molecule was present in the asymmetric unit. All the non-hydrogen atoms were refined anisotropically. The final full-matrix least-squares refinement converged with $R = 0.066$ and $R_w = 0.087$. The maximum and minimum peaks on the final difference Fourier map corresponded to 0.68 and −0.73 e $Å^{-3}$.

Orange platelike crystals of **3**·2EtOH suitable for X-ray crystallographic study were grown by evaporation from a CH_2Cl_2/EtOH solution. A crystal was selected, mounted on a glass fiber, and quickly coated with an epoxy resin in order to avoid contact with the air, since the crystal quality was sensitive to the loss of solvent. As well as the copper-containing molecule, the asymmetric unit contains a molecule of EtOH and also a two-atom fragment which gave a four-atom fragment upon expansion about a center of symmetry and was considered to be a disordered EtOH molecule. The non-hydrogen atoms were refined anisotropically, except those of the disordered EtOH molecule, which were refined isotropically. The final full-matrix least-squares refinement converged with $R = 0.084$ and $R_w = 0.092$. The maximum and minimum peaks on the final difference Fourier map corresponded to 0.74 and −0.69 e$Å^{-3}$.

Physical Measurements. The ^1H NMR spectrum of BimOBz was recorded on a Bruker AC 300 spectrometer. Mass spectra using EI and CI ionisation were obtained using an IC Kratos MC25 instrument; +FAB spectra were recorded on a Kratos Concept 1S spectrometer. Electronic spectra were recorded on a Shimadzu UV-260 spectrometer; electronic spectra of solid samples were obtained by reflectance with a finely ground sample of the compound using $BaSO_4$ (99.7%) as both the reference and the base material onto which the sample was loaded. EPR spectra were recorded on a Varian E112 spectrometer at X- and Q-band frequencies. Cyclic voltammetric studies were performed using an EG&G PAR 173 potentiostat and universal programmer. A glassy carbon working electrode, platinum wire secondary electrode, saturated calomel reference electrode (SCE), and the electrolyte $[NBu^n{}_4][BF_4]$ were used in the cell.

Results and Discussion

Synthesis and Structure. The synthesis of imidazole chelates as chemical analogs for the histidine side chain has led us to synthesize a series of poly(imidazole) chelates.[19−21] The synthesis of BimOBz is a result of earlier investigation of the copper chemistry of the precursor ligand BimOH. These investigations demonstrated that the alcohol functionality of BimOH was capable of deprotonating in the presence of copper and resulted in the formation of alkoxide bridged copper clusters. Thus, conversion of the alcohol group to an ether functionality was considered desirable to promote the synthesis of monomeric copper compounds. The synthesis of BimOBz involved treating the sodium salt of BimOH with benzyl bromide at room temperature (Scheme 1). Subsequent coordination chemistry of BimOBz resulted in the synthesis of the monomeric copper complexes $[Cu(BimOBz)_2][BF_4]_2$ (**1**), $[Cu(BimOBz)(NO_3)_2]$ (**2**), and $[Cu(BimOBz)Cl_2]$ (**3**), which have been characterized by crystallography. The coordination geometry of the copper centers of these compounds are presented in Tables 2−4 .

Table 2. Selected Bond Distances (Å) and Angles (Deg) (and ESDs) of **1**·solv

Bond Distances			
Cu1−N1	1.94(1)	Cu1−N3	2.02 (1)
Cu1−N5	2.00(1)	Cu1−N7	1.92 (1)
Bond Angles			
N1−Cu1−N3	93.7(6)	N1−Cu1−N5	105.2(6)
N1−Cu1−N7	142.9(6)	N3−Cu1−N5	117.0(6)
N3−Cu1−N7	105.5(6)	N5−Cu1−N7	94.1(6)

Table 3. Selected Bond Distances (Å) and Angles (Deg) (and ESDs) of **2**·CH_2Cl_2

Bond Distances			
Cu1−N1	1.997(4)	Cu1−N3	1.966(4)
Cu1−O2	1.968(4)	Cu1−O5	2.006(4)
Cu1−O3	2.603(4)	Cu1−O6	2.492(4)
Bond Angles			
O2−Cu1−O5	86.9(2)	O2−Cu1−N1	92.9(2)
O2−Cu1−N3	174.5(2)	O5−Cu1−N1	165.1(1)
O5−Cu1−N3	90.3(2)	N1−Cu1−N3	91.0(2)

Table 4. Selected Bond Distances (Å) and Angles (Deg) (and ESDs) of **3**·2EtOH

Bond Distances			
Cu1−Cl1	2.212(3)	Cu1−Cl2	2.245(3)
Cu1−N1	1.997(7)	Cu1−N3	1.989(7)
Bond Angles			
Cl1−Cu1−Cl2	104.9(1)	Cl1−Cu1−N1	103.9(2)
Cl1−Cu1−N3	132.5(2)	Cl2−Cu1−N1	125.8(2)
Cl2−Cu1−N3	100.0(2)	N1−Cu1−N3	92.9(3)

1·solv consists of monomeric $[Cu(BimOBz)_2]^{2+}$ cations (Figure 1) and $[BF_4]^-$ anions. Each copper has a CuN_4 coordination (Cu−N1 1.94(1) Å, Cu1−N3 2.02(1) Å, Cu1−N5 2.00(1) Å, Cu1−N7 1.92(1) Å), resulting from the ligation of two BimOBz ligands. The angles associated with coordination sphere (N1−Cu1−N3 93.7(6)°, N1−Cu1−N5 105.2(6)°, N1−Cu1−N7 142.9(6)°, N3−Cu1−N5 117.0(6)°, N3−Cu1−N7 105.5(6)°, N5−Cu1−N7 94.1(6)°) indicate that the geometry of the CuN_4 unit is considerably removed from square-planar with the interligand dihedral angle (ω) between the Cu1, N1, N3 and Cu1, N5, N7 planes being 73.0°. The bite angles of the ligands, N1−Cu1−N3 93.7(6)° and N5−Cu1−N7 94.1(1)°, impose one of the constraints upon the geometry. Another governing factor is the presence of considerable steric bulk of the ligands; the ligands appear to adopt a conformation in which the intramolecular steric interactions, most notably those between phenyl groups on the 4-positions of the imidazole groups, are minimized.

A comparison of the geometry of the Cu^{II} ion in **1** with other $[Cu(bis(imidazole))_2]^{2+}$ complexes is presented in Table 5. The similarity of the interligand dihedral angle, ω, and the average intraligand angle, *D*, indicate that the geometry of the Cu^{II} ion in **1** is similar to that found in $[Cu(BimKet)_2]^{2+}$ (BimKet = bis(1-methyl-4,5-diphenylimidaz-2-oyl)ketone).[20] The value of the ω (86.3°) in $[Cu(BiPhen)_2]^{2+}$ (BiPhen = 2,2′-bis(2-imida-

---

(25) Spek, A. L. *Acta Crystallogr.* **1990**, *A46*, C34.

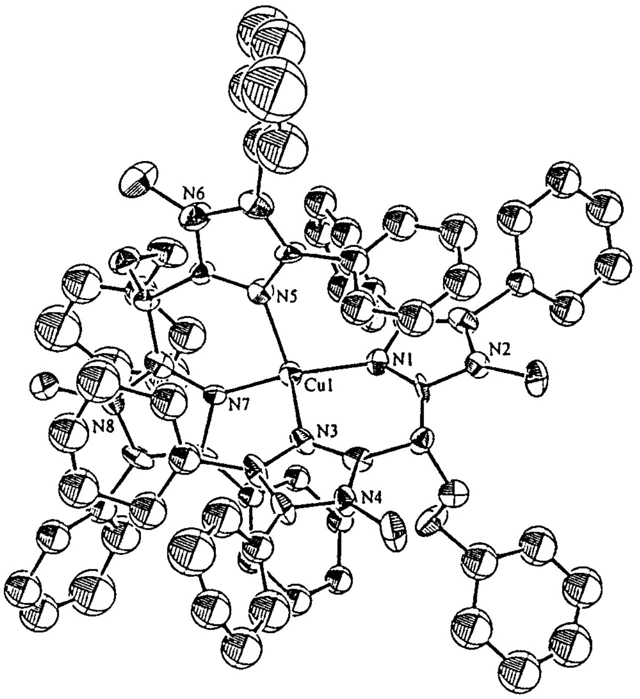

Figure 1. ORTEP view of $[Cu(BimOBz)_2]^{2+}$. The 30% probability ellipsoids are shown, and selective atomic labeling has been used.

Table 5. Comparison of the Geometry of the Cu^{II} Ion and Copper Hyperfine Coupling Constants in a Selection of $[Cu(bis(imidazole))_2]^{2+}$ Complexes

			$A_z^b/10^{-4}$ cm^{-1}			
ligand	ω^a/deg	D^a/(deg)	solid	CH_2Cl_2	MeCN	ref
BimOBz	73.0	93.9	94	104	107	*c*
BimKet	68.2	94.2	112	114	121	20
BiPhen	86.3	141.9	130	*d*	147	26

[a] ω, interligand dihedral angle; *D*, average intraligand angle. [b] EPR spectra recorded at 77 K. [c] This work. [d] Not available.

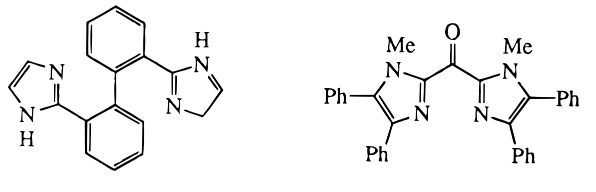

BiPhen BimKet

Figure 2. Bis(imidazole) ligands BiPhen[26] and BimKet.[20]

zoyl)biphenyl) infers that the Cu^{II} center in this compound is very close to tetrahedral.[26] However, the value of *D* for $[Cu(BiPhen)_2]^{2+}$ (141.9°) indicates a greater distortion toward square-planar than that of both **1** and $[Cu(BimKet)_2]^{2+}$, and this is reflected in the electronic properties of this compound (*vide infra*).

2·CH_2Cl_2 (Figure 3) is comprised of monomeric $[Cu(BimOBz)(NO_3)_2]$ units, in each of which Cu^{II} is coordinated to two imidazole groups from the bis(imidazole) ligand (Cu1−N1 1.997(4) Å, Cu1−N3 1.966(4) Å) and two nitrate groups. According to the criteria suggested by Reedijk *et al.*,[27] the nitrato group N6,O2,O3,O4 binds as a unidentate ligand to the copper (Cu1−O2 1.968(4) Å, Cu−O3 2.603(4) Å), whereas the other nitrato group is anisobidentate (Cu1−O5 2.006(4) Å, Cu1−O6 2.492(4) Å). Therefore, strictly speaking, the Cu^{II} is five-coordinate (CuN_2O_3). However, since Cu1−O6 is relatively long, the primary coordination of the Cu^{II} can be approximated to CuN_2O_2, the geometry of which is almost square-planar. N1−Cu1−N3 (91.0(2)°), O2−Cu1−O5 (86.9(2)°), O5−Cu1−N3 (90.3(2)°), and O2−Cu1−N1 (92.9(2)°) each approach 90°, and O2−Cu1−N3 (174.5(2)°) and O5−Cu1−N1 (165.1(1)°) approach 180°; the dihedral angle between the CuN_2 and CuO_2 planes is 15.6°. The imidazole rings are twisted away from the CuN_2 plane; the dihedral angle between CuN_2 plane and imidazole rings N1,C2,N2,C3,C4 and N3,C18,N4,C19,C20 are 35.9 and 27.5°, respectively. The dihedral angle between the imidazole groups within the ligand is 32.1°. The nitrato groups are almost mutually perpendicular with a dihedral angle of 77.7°.

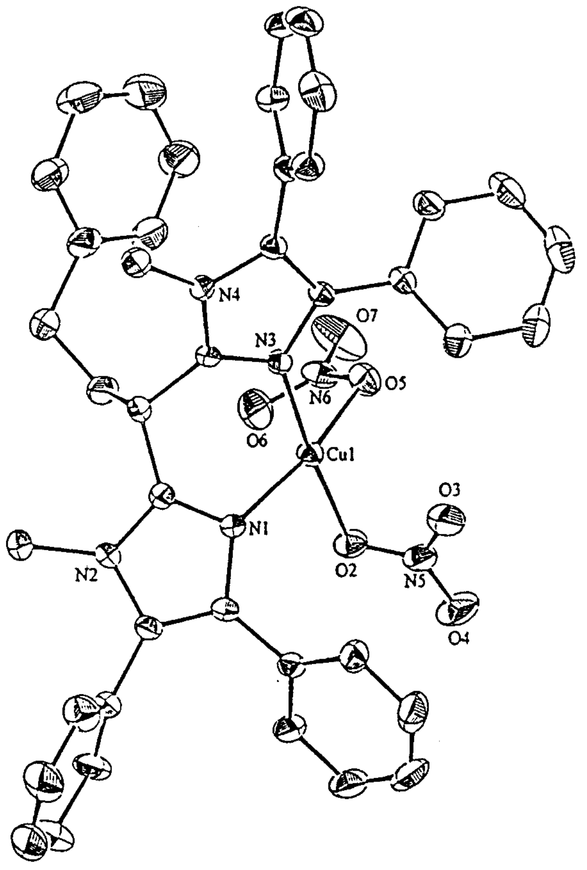

Figure 3. ORTEP view of $[Cu(BimOBz)(NO_3)_2]$. The 30% probability ellipsoids are shown, and selective atomic labeling has been used.

3·2EtOH (Figure 4) consists of monomeric $[Cu(BimOBz)Cl_2]$ units in which each copper atom is coordinated to two imidazole nitrogens (Cu1−N1 1.997(7) Å, Cu1−N3 1.989(7) Å) from BimOBz and to two chlorine atoms (Cu1−Cl1 2.212(3) Å, Cu1−Cl2 2.245(3) Å). The geometry of the CuN_2Cl_2 unit is intermediate between square-planar and tetrahedral. The angles associated with the coordination sphere of the Cu^{II} (N1−Cu1−N3 92.9(3)°, N1−Cu1−Cl1 103.9(2)°, N1−Cu1−Cl2 125.8(2), N3−Cu1−Cl1 132.5(2)°, N3−Cu1−Cl2 100.0(2), Cl1−Cu1−Cl2 104.9(1)°) and the dihedral angle between the CuN_2 and $CuCl_2$ planes (68.5°) indicates that the coordination geometry is closer to tetrahedral than square-planar. The imidazole rings are twisted away from the CuN_2 plane; the dihedral angle between the CuN_2 plane and the imidazoles N1,C2,N2,C3,C4 and N3,C18,N4,C19,C20 are 15.1 and 12.8°, respectively. The dihedral angle between the imidazole groups within the ligand is 22.8°.

---

(26) Knapp, S; Keenen, T. P.; Zhang, X; Fikar, R; Potenza, J. A.; Schugar, H. J. *J. Am. Chem. Soc.* **1990**, *112*, 3452.

(27) Kleyweg, G. J.; Wiesmeijer, W. G. R.; Van Driel,G. J.; Driessen, W. L.; Reedijk, J.; Noordik, J. H. *J. Chem. Soc., Dalton Trans.* **1985**, 2177.

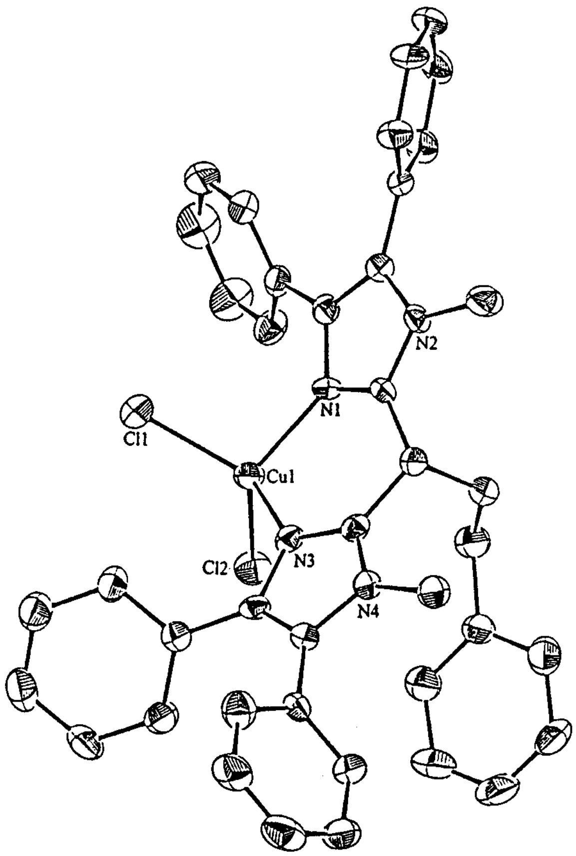

Figure 4. ORTEP view of [Cu(BimOBz)Cl_2]. The 30% probability ellipsoids are shown, and selective atomic labeling has been used.

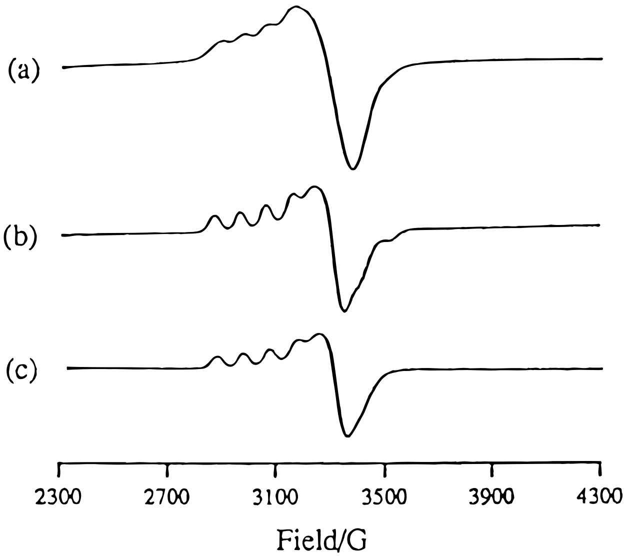

Figure 5. X-band EPR spectra of **1**: (a) powder at 298 K; (b) in CH_2Cl_2 at 77 K; (c) in MeCN at 77 K.

Electronic Structure. The X- and Q-band powder and frozen glass EPR spectra of **1** (Figure 5) are rhombic and characteristic of CuN_4 complexes with a d_{xy} ground state.[28] The X-band powder spectrum, recorded at both room temperature and 77 K, shows $^{63,65}Cu$ hyperfine splitting in the g_z region; three of the four lines are easily observed and the fourth is partially hidden in the $g_{x,y}$ region. All four Cu hyperfine lines are observed in the Q-band powder spectrum ($g_x = 2.06$, $g_y = 2.13$, $g_z = 2.30$, $A_z = 94 \times 10^{-4}$ cm^{-1}). The metal hyperfine coupling constant, A_z, of **1** increases in CH_2Cl_2 and MeCN (recorded at 77 K), indicating that the geometry at the copper center becomes less tetrahedral in solution; however, this difference is small ($<13 \times 10^{-4}$ cm^{-1} in MeCN), suggesting that the solid state structure is essentially retained in solution. The metal hyperfine splittting value of **1** as both a solid and frozen glass ($A_z < 110 \times 10^{-4}$ cm^{-1}) is considerably smaller than those observed for other $[Cu(imidazole)_4]^{2+}$ centers.[19,21a,29] In fact, the value of A_z in **1** is even smaller than that for the near tetrahedral CuN_4 compounds $[Cu(BimKet)_2][BF_4]_2$[20] and $[Cu(BiPhen)_2][ClO_4]_2$.[26] This observation is significant because studies have demonstrated that the value of A_z in compounds with CuN_4 centers decreases as the distortion from square-planar to tetrahedral increases.[30] This correlation between the inter-ligand dihedral angle, ω, and A_z is in the sense that as ω increases A_z decreases. On this basis, it seems surprising that the value of A_z in $[Cu(BiPhen)_2][ClO_4]_2$ ($\omega = 86.3°$, $A_z = 130 \times 10^{-4}$ cm^{-1})[26] is greater than that found in **1** ($\omega = 73.0°$, $A_z = 94 \times 10^{-4}$ cm^{-1}) and $[Cu(BimKet)_2][BF_4]_2$ ($\omega = 68.2°$, $A_z = 112 \times 10^{-4}$ cm^{-1}).[20] However, this correlation does not take account of the intraligand angles which are substantially larger in $[Cu(BiPhen)_2][ClO_4]_2$ (141.9°) than in **1** (93.9°) and $[Cu(BimKet)_2][BF_4]_2$ (94.2°), and this will affect the electronic structure of the Cu^{II} center.

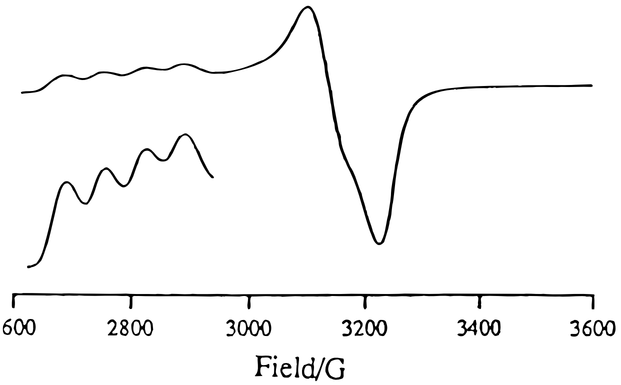

Figure 6. X-band EPR spectrum of **3** in CH_2Cl_2 at 77 K.

The EPR powdered X- and Q-band spectra of **2** are axial in character ($g_{x,y} = 2.06$, $g_z = 2.28$); three of the four metal hyperfine peaks are observed at X-band, and all are seen at Q-band. The value of the metal hyperfine splitting ($A_z = 169 \times 10^{-4}$ cm^{-1}) is typical of that observed for Cu^{II} in an essentially planar environment.[28]

A full analysis of the X- and Q-band powder EPR spectra of **3** at room temperature (and 77 K) was not possible because of line-broadening, but $g_{x,y} = 2.08$, $g_z = 2.38$ were read from the Q-band spectrum. The X-band spectrum of **3** in CH_2Cl_2 at 77 K gave $g_{x,y} = 2.06$ and $g_z = 2.37$ with all four of the Cu hyperfine lines apparent in the g_z region (Figure 6); the A_z value of 75×10^{-4} cm^{-1} is even lower than that observed in the EPR spectrum of **1** in CH_2Cl_2 at 77 K. The geometries of the Cu^{II} center in both **1** and **3** are similar (distorted tetrahedral), and the additional decrease in the metal hyperfine value of **3** may be attributed to the covalency of the Cu−Cl bonds.

The UV−visible spectra of **1**−**3** are presented in Table 6. The assignments of the bands in the spectra of these complexes were made by comparison with the UV−visible spectra of the free ligand ($\pi \rightarrow \pi^*$, $\nu = 37\,700-37\,400$ cm^{-1}) and [Cu-

---

(28) Mabbs, F. E.; Collison, D. *Electron Paramagnetic Resonance of d-Transition Metal Complexes*; Elsevier: Amsterdam, 1992.

(29) Prochaska, H. J.; Scwindinger, W. F.; Schwartz, M.; Burk, M. J.; Bernarducci, E; Lalancette, R. A.; Potenza, J. A., Schugar, H. J. *J. Am. Chem. Soc.* **1981**, *103*, 3446.

(30) Addison, A. W. In *Copper Chemistry: Biochemical and Inorganic Perspectives*; Karlin, K. D., Zubieta, J., Eds.; John Wiley & Sons: New York, 1983, p 109.

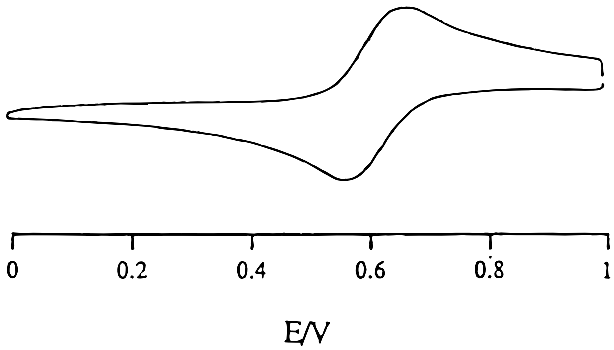

Figure 7. Cyclic voltammogram of a 1 mM solution of $[Cu(BimOBz)_2][BF_4]_2$ recorded at 298 K in a 0.2 M solution of $[NBu^n{}_4][BF_4]$ in CH_2Cl_2 using a glassy carbon electrode, a scan rate of 200 mV s^{-1}, and an SCE reference electrode.

Table 6. Electronic Absorption Spectra with Band Assignments for **1**−**3**

	ν/cm^{-1} ($\epsilon/M^{-1}\ cm^{-1}$)		
CH_2Cl_2	MeCN	solid	assignment
	Compound **1**		
38 800 (69 400)	38 600 (60 500)	38 200	$\pi \rightarrow \pi^*$
26 200 (1930)	27 100 (1910)	25 400	im → Cu LMCT
16 050 (227)	16 900 (267)	15 900	*d*−*d*
12 400 (202)	12 600 (202)	12 200	*d*−*d*
	Compound **2**		
38 900 (39 300)	39 400 (42 800)	37 900	$\pi \rightarrow \pi^*$
		25 500	im → Cu LMCT
15 400 (56)	16 600 (45)	16 300	*d*−*d*
13 300 (61)	13 700 (61)	14 000	*d*−*d*
	Compund **3**		
37 900 (39 700)	37 800 (36 200)	37 300	$\pi \rightarrow \pi^*$
25 100 (1230)	25 500 (1021)	24 600	im → Cu LMCT
18 350 (74)		18 250	*d*−*d*
11 400 (76)	11 100 (81)	11 500	*d*−*d*

$(imidazole)_4]^{2+}$ complexes.[19−21a,26,31,32] The similarity of the the solid and solution UV−visible spectra of these complexes indicates that the solid state structures of **1**−**3** are essentially retained in CH_2Cl_2 and MeCN solution.

Electrochemistry. A cyclic voltammogram for **1** in CH_2Cl_2 over the potential range 0 to +1.0 V at a scan rate of 200 mV s^{-1} is presented in Figure 7. Analysis over this range at a variety of scan rates (500−50 mV s^{-1}) showed the presence of a redox process at +0.62 V in CH_2Cl_2 and +0.49 V in MeCN vs a SCE, respectively, which is assigned to the $[Cu(BimOBz)_2]^{2+}/[Cu(BimOBz)_2]^+$ couple. The ratio of $i_p{}^c/i_p{}^a$ over the scan rates 500−50 mV s^{-1} is ~1 in both CH_2Cl_2 and MeCN; the peak−peak separation, ΔE, decreased from 110 mV at 500 mV s^{-1} to 80 mV at 50 mV s^{-1} in CH_2Cl_2; ΔE decreased from 90 mV at 500 mV s^{-1} to 70 mV at 50 mV s^{-1} in MeCN; a plot of $i_p{}^c$ vs $\nu^{1/2}$ is a straight line for both solvents. Under identical conditions, the cyclic voltammogram of ferrocene displayed a reversible couple in both CH_2Cl_2 and MeCN with $\Delta E = 70$ mV. Therefore, the $[Cu(BimOBz)_2]^{2+}/[Cu(BimOBz)_2]^+$ couple may be described as reversible.[33]

The reversibility of the $[Cu(BimOBz)_2]^{2+}/[Cu(BimOBz)_2]^+$ couple can be rationalized on the basis that the geometry of the copper center in **1** is a flattened tetrahedral, a geometry that could accommodate Cu^I;[34] i.e., electron transfer between the Cu^{II} and Cu^I states should not require a significant reorganization of the metal. $[Cu(BimOBz)_2]^+$ has been synthesized electrochemically; reduction of $[Cu(BimOBz)_2]^{2+}$ at +0.1 V (in both CH_2Cl_2 and MeCN) resulted in the decoloration of the green/blue solution to produce a colorless solution over a period of 1 h at room temperature. The cyclic voltammogram of the colorless solution was identical to that of the Cu^{II} complex. Oxidation to the Cu^{II} derivative was achieved rapidly, either by controlled-potential electrolysis at a potential of +1.0 V under an inert atmosphere or by exposure to air.

Table 7. Comparison of the Redox Potentials of a Selection of $[Cu(bis(imidazole))_2]^{2+}$ Complexes

ligand	ω^a/deg	D^a/deg	$E°$ (CH_2Cl_2)/V	$E°$ (MeCN)/V	ref
BimOBz	73.0	93.9	0.62	0.49	this work
BimKet	68.2	94.2	0.80	0.59	20
BiPhen	86.3	141.9	*b*	0.11	26

[a] ω, interligand dihedral angle; *D*, average intraligand angle. [b] Not available.

Examples of reversible Cu^{II}/Cu^I redox couples of CuN_4 complexes are rare[20,26] since $Cu^{II}N_4$ centers generally tend to adopt a square-planar geometry and Cu^IN_4 centers favor tetrahedral geometry.[34] Table 7 presents a comparison of the redox potential of the Cu^{II}/Cu^I couple and the overall geometry of **1** with those for two other $[Cu(bis(imidazole))_2]^{2+}$. The positive redox potential of the $[Cu(BimOBz)_2]^{2+}/[Cu(BimOBz)_2]^+$ couple is attributed to the geometry of the Cu^{II} center, for which interligand steric interactions prevent adoption of a tetragonal geometry, and to the presence of ligands which are capable of being π-acceptors. Thus, although the geometry of the the Cu center in $[Cu(BimKet)_2]^{2+}$ is similar to that of **1**, the more positive redox potential of the former may be a result of an increased π-acceptor ability of the BimKet ligand, arising from the extended conjugation of this ligand.

Conclusion

The syntheses of a new sterically hindered imidazole chelate (BimOBz) and three monomeric copper(II) complexes have been achieved. The coordination number at the copper center has been resticted to four by the use of this sterically hindered ligand. Furthermore, we have shown that the small values of copper hyperfine splitting and high redox potentials, characteristic of type I copper proteins, can be reproduced by complexes of alkylated imidazole ligands without the presence of thiolate coordination. Thus, **1** and **3** have Cu hyperfine splitting (A_z) values of 94 × 10^{-4} and 75 × 10^{-4} cm^{-1}, respectively. **1** displays a reversible, one-electron Cu^{II}/Cu^I couple in CH_2Cl_2 and MeCN at potentials of +0.62 and +0.49 V vs SCE, respectively. The reversibility of the $[Cu(BimOBz)_2]^{2+}/[Cu(BimOBz)_2]^+$ couple demonstrates that electron transfer proteins could possess a $[Cu(histidine)_4]$ core.

Acknowledgment. We thank the University of Manchester for the provision of a scholarship (R.B), the funds provided by the EC Human Capital and Mobility Framework III MASIMO Network, and Drs. T. C. Higgs, J. McMaster, D. Collison, and E. J. L. McInnes for their valuable contributions.

Supporting Information Available: Three X-ray crystallographic files, in CIF format, are available on the Internet only. Access information is given on any current masthead page.

IC961204C

---

(31) Bernarducci, E; Bharadawaj, P. K.; Lalancette, R. A.; Krogh-Jesperson, K; Potenza, J. A., Schugar, H. J. *Inorg. Chem.* **1983**, *22*, 3911.

(32) Bernarducci, E; Bharadawaj, P. K.; Krogh-Jesperson, K.; Potenza, J. A.; Schugar, H. J. *J. Am. Chem. Soc.* **1983**, *105*, 3860.

(33) Southampton Chemistry Group. *Instrumental Methods in Electrochemistry*, John Wiley & Sons: New York, 1985.

(34) Hathaway, B. J.; Billing, D. E. *Coord. Chem. Rev.* **1970**, *5*, 143.